Available online at www.sciencedirect.com
SCIENCE DIRECT®
Journal of Solid State Chemistry 177 (2004) 1219–1229
JOURNAL OF SOLID STATE CHEMISTRY
http://elsevier.com/locate/jssc

Neutron diffraction study of the deuterides of the over-stoichiometric compounds $LaNi_{5+x}$

M. Latroche,[a,*] J.-M. Joubert,[a] A. Percheron-Guégan,[a] and F. Bourée-Vigneron[b]

[a] *Lab. de Chimie Mettall. des Terres Rares, Centre National de la Recherche Science, CNRS, 2 Rue Henri Dunant, Thiais Cedex F-94320, France*
[b] *Laboratoire Léon Brillouin, CE-Saclay, Gif-sur-Yvette F-91191, France*

Received 1 August 2003; received in revised form 24 October 2003; accepted 26 October 2003

Abstract

The deuterides of three intermetallic compounds $LaNi_{5+x}$ with $x = 0$, 0.2 and 0.4 have been prepared and analyzed by neutron powder diffraction at two different deuterium concentrations. On one hand, the crystallographic properties of the α and the β phases have been studied with the two phases in equilibrium on the pressure plateau characteristic for the phase transition. On the other hand, the β phase has been studied as a single phase in the solid solution domain. Crystal structures were refined using the Rietveld method. Crystal symmetry, lattice parameters and deuterium sites and occupancy parameters are reported for all the different phases. Anisotropic line profile analysis has been used to characterize the strains induced by deuterium absorption in the various regions of the Pressure–Composition–Isotherm curves. Results are compared for the different values of x and related to the cycle life properties for each compound.

Keywords: Intermetallics; Hydrogen storage materials; Gas–solid reaction; Crystal structure; Neutron diffraction; Over-stoichiometry; $LaNi_5$

1. Introduction

Many AB_5 compounds (A: rare earth, B: transition metal) with the $CaCu_5$ structure type ($P6/mmm$ space group, A in $1a$, B in $2c$ and $3g$) are known to store reversibly large amounts of hydrogen and the obtained metallic hydrides can be used in various applications like Ni-MH batteries, spacecraft cryo-coolers or fuel cell supply tanks. However, long-term cycling leads to severe degradation of the material [1]. It has been shown that the alloy cycling stability can be significantly improved by employing the so-called non-stoichiometric compounds [2–5]. For example, over-stoichiometric samples exhibit enhanced electrochemical cycle life and long-term cycling can be achieved with Cu or Mn substituted over-stoichiometric electrode materials [6].

The existence of a homogeneity domain for $LaNi_{5+x}$ at high temperature ($-0.1 \leqslant x \leqslant 0.40$ at 1543 K) has been reported by several authors [7,8]. For the nickel-poor (under-stoichiometric) compositions, random substitutions of Ni by La were originally proposed to explain the non-stoichiometry but more recent work proposes a lower limit of $LaNi_{4.88}$ and assumed the simultaneous occurrence of both lanthanum atoms and vacancies on the nickel sites [9]. The over-stoichiometry in $LaNi_{5+x}$ has been interpreted by the presence of randomly distributed nickel atom dumbbells occupying site $2e$ in $P6/mmm$ space group oriented along the c-axis and replacing lanthanum atoms. Moreover, the Ni atoms forming a hexagon in the $z = 0$ plane around the dumbbell are no longer on site $2c$ but shrink into position $6\ell (x < 1/3)$. This structural hypothesis has been confirmed by several diffraction studies [9–11]. Accordingly, the stoichiometry is better described with the formula $La_{1-y}Ni_{5+2y}$ $y = x/(7+x)$ that describes the real number of atoms lying in the crystallographic cell.

The over-stoichiometry is limited to $x = 0.4$ in the equilibrium diagram of the binary La–Ni system. However, recent works have shown that highly over-stoichiometric compounds ($1 \leqslant x \leqslant 4$) (so-called "*super*" stoichiometric) can also be obtained using non-equilibrium methods [12,13]. Crystallographic and thermodynamic properties of $LaNi_{5+x}D_{4.9}$ with $x \approx 1$ have been reported in Ref. [14]. However, in situ neutron diffraction analysis of this latter compound did not allow to

*Corresponding author. Fax: +33-0-1-49-78-12-03.
E-mail address: latroche@glvt-cnrs.fr (M. Latroche).

0022-4596/$ - see front matter © 2003 Elsevier Inc. All rights reserved.
doi:10.1016/j.jssc.2003.10.029

fully determining the deuterium atom location since data were collected on a low-resolution diffractometer.

The structure of the hydride of the stoichiometric compound $LaNi_5H_{6.6}$ has been subject to a lot of controversy. Lartigue and co-workers [15] carefully investigated the structure at different D concentrations from 5 to 6.7 D/mol. The low concentrated β phase could be described either in $P6/mmm$ or $P6mm$ space groups with 5 or 4 deuterium sites, respectively. Increasing the concentration, they found that the deuteride undergoes a structural phase transformation due to a progressive ordering of D atoms. This results in a reduction of symmetry and in a superstructure leading to a doubling of the c-axis and to a new description in space group $P6_3mc$ with seven interstitial sites for deuterium. At the same time, Thompson et al. [16] studied an isotopically enriched ^{60}Ni compound to enhance the D scattering contribution and confirmed the superstructure leading to a double hexagonal cell for the saturated deuteride.

To our knowledge, few works have been devoted to the structural properties of $LaNi_{5+x}$ hydrides and structural investigations of the deuterides of the over-stoichiometric compounds have not been reported yet. In the present work, we report on the structural properties of the deuterides $LaNi_{5+x}D_y$ ($x = 0$; 0.2 and 0.4) studied by powder neutron diffraction (ND) analysis. Space group, symmetry and cell parameters have been determined and crystallographic properties are discussed as a function of x in relation with the nature and occupancy factors of the deuterium sites. Anisotropic line broadening has also been investigated for each phase as a function of the deuterium composition on both sides of the equilibrium plateau.

2. Experimental

Three intermetallic samples (with $x = 0$, 0.2 and 0.4) were prepared by induction or arc melting of the pure components (3N purity) under argon in a water-cooled copper crucible. The samples were melted five times to ensure good homogeneity. They were then annealed at 1200°C for 4 days and quenched to room temperature. Details about preparation of over-stoichiometric samples are given in Ref. [9]

Metallographic examination and elemental analysis by electron probe micro-analysis (EPMA Cameca SX100) were performed to check the homogeneity and stoichiometry of the alloys. The powder X-ray diffraction experiments (XRD) were obtained at room temperature on a Bruker AXS D8 $\theta-\theta$ diffractometer using Cu$K\alpha$ radiation (Bragg-Brentano geometry, 2θ-range 20–120°, step size 0.02°, backscattered rear graphite monochromator). All the patterns were indexed in the $CaCu_5$-type hexagonal cell ($P6/mmm$ space group) and refined with the Rietveld method using the program FULLPROF [17].

Pressure composition isotherm (PCI) curves were measured with deuterium gas using the Sievert's method at room temperature. For powder ND analysis, about 8 g of crushed alloys were activated by five deuterium absorption–desorption cycles, transferred to a silica tube sample holder for the last absorption, deuterium saturated to a pressure of about 10 bar (see Table 1) and closed under pressure to prevent any desorption during ND pattern acquisition. For the measurement of α and β phases in equilibrium (so-called mid plateau measurements), two saturated samples (with $x = 0.2$ and 0.4) were desorbed to a nominal capacity of about 3D/f.u. The sample with nominal capacity $LaNi_5D_{2.95}$ was obtained by deuterium gas absorption on the fully desorbed sample. Detailed values for all prepared deuterides are given in Table 1.

ND measurements were carried out at the Laboratoire Léon Brillouin in Saclay. The diffraction patterns were recorded at room temperature on the 3T2 instrument in the range $6° < 2\theta < 120°$ by step of 0.05° ($\lambda = 1.225$ Å). The wavy background generated by the silica tube sample holder was taken into account by interpolation. According to previous works, three different structural models were tested for the description of the deuterides. The first one keeps the cell and symmetry of the intermetallic compound ($P6/mmm$ space group with La in 1a, Ni in 2c, 3g, 6l and 2e). The four different crystallographic sites containing deuterium atoms are given in Table 3. The second model corresponds to a description in $P6mm$ space group for which the mirror perpendicular to the c-axis is

Table 1
Capacity and absorption pressure (or desorption pressure) for the different studied deuterides

Over-stoichiometry x	Nominal formula unit	Mid plateau deuteride (bar)	Saturated deuteride (bar)
0.0	$LaNi_{5.0}$	2.95 D/f.u. 2.90	6.5 D/f.u. 11.56
0.2	$La_{0.97}Ni_{5.06}$	3.00 D/f.u. 2.81[a]	5.9 D/f.u. 9.75
0.4	$La_{0.95}Ni_{5.11}$	2.98 D/f.u. 4.04[a]	5.45 D/f.u. 8.70

All the deuterium capacities are referred to $La_{1-y}Ni_{5+2y}$ formula unit.
[a] Desorption pressure.

lost (La in 1*a*, Ni in 2*b*, 3*c*, 6*e*, $1a_1$ and $1a_2$) [15]. The four D sites of the *P*6/*mmm* model split into seven ones. In our refinements, the *z* positions of the D atoms were kept constrained in such a way that the loss of the mirror affects only the occupation ratio of the sites on each side of the mirror, but not their relative position. However, in the last stage of the refinement, the *z* position of the lanthanum (0,0,*z*) was refined leading to a small shift of this latter atom above the *ab* plane. The third model corresponds to a cell twice larger obtained from a doubling of the *c*-axis in space group $P6_3mc$ (La in 2*a*, Ni in $2a_1$, $2a_2$, $2b_1$, $2b_2$, 6*c*, $6c_1$, $6c_2$) [15,18]. In this double cell, the four sites of the original cell split into 12 different structural positions for the deuterium atoms as shown in Table 3. However, according to Lartigue et al. [15], only seven sites are found occupied. Again despite the symmetry lowering in space group $P6_3mc$, *z* atomic positions of the D atoms were kept constrained as shown in Table 3 and occupancy factors for each site were refined independently. A schematic view of the three different models is shown in Fig. 1. For sake of clarity, the figure does not show realistic *x* and *y* positions but describes the stacking of the deuterium atoms along the *c*-axis. Finally, as previously reported by several authors, important anisotropic broadening occurs upon cycling and full refinement of the powder pattern cannot be performed using an isotropic profile function. Anisotropic line broadening can be described using two parameters S_{AA} and S_{CC} that represent the amount of strains in the basal plane and along the *c*-axis of the hexagonal cell respectively. The isotropic contribution to the line width was fixed to that of the instrument. Such an approach has already been discussed in previous works [19,20] and has been used again in the present study.

3. Results

Characterization of the intermetallic samples shows that all compounds are single phase and homogeneous except for $LaNi_{5.4}$ for which small peaks corresponding to FCC Ni solid solution are present in the diffraction pattern (quantity evaluated to 1.9 wt%). Analysis of the XRD data shows that the parameter *a* decreases with *x* whereas the parameter *c* increases. The resulting cell volume decreases as a function of the over-stoichiometry. Peculiar attention has been paid to the determination of the actual over-stoichiometry of our samples. As the number of electrons of lanthanum atoms (57) is close

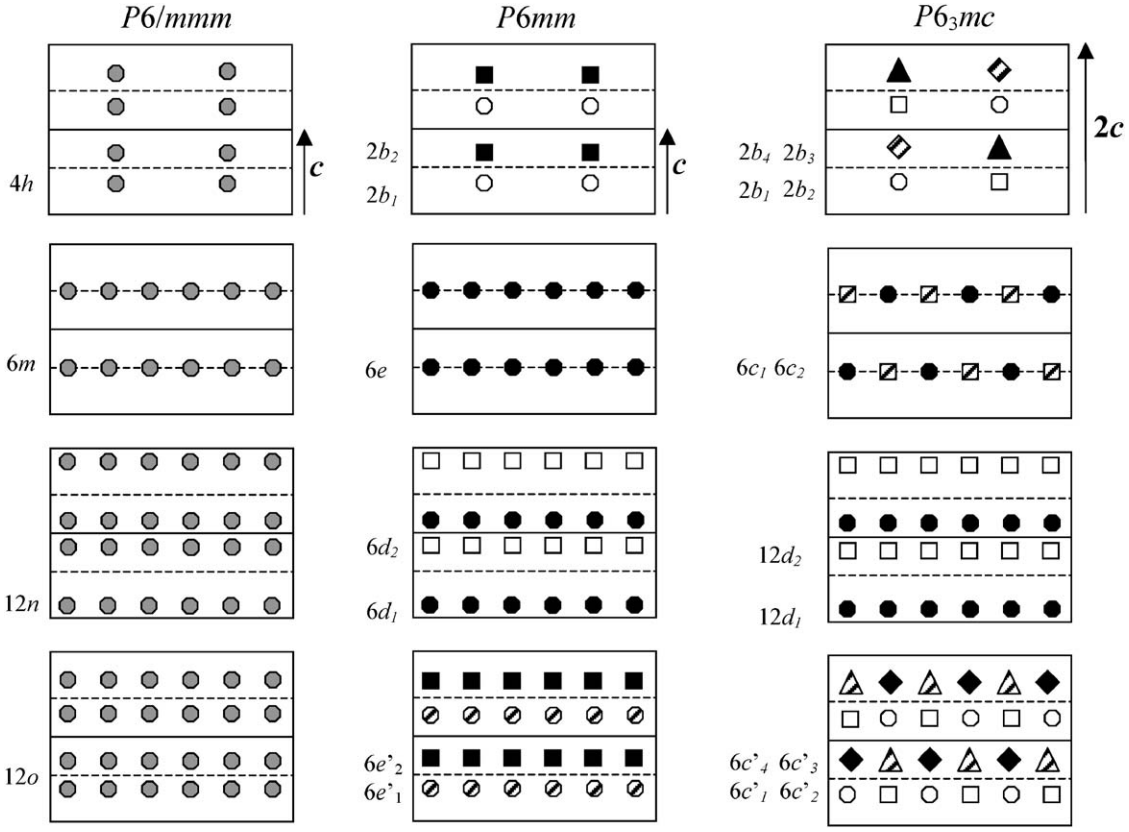

Fig. 1. Schematic view for the different repartitions of the deuterium atoms in the three different space groups (*P*6/*mmm*, *P*6*mm*, $P6_3mc$). For sake of clarity, the figure does not show realistic *x* and *y* positions but only describes the stacking of the deuterium atoms along the *c*-axis. The different symbols stand for different Wyckoff positions according to the given space group. Symbol style means empty (white), poorly occupied (hatched) or partially filled (black) deuterium sites.

Table 2
Cell parameters, volume and over-stoichiometry for the different intermetallic compounds

Nominal x	Nominal formula unit	Measured over-stoichiometry x		Cell parameters (XRD)(± 0.0004 Å)		
	$La_{1-y}Ni_{5+2y}$	EPMA	Estimated from cell parameters[a]	a (Å)	c (Å)	V (Å^3)
0.0	$LaNi_{5.0}$	−0.04	0.03	5.0157	3.9823	86.76
0.2	$La_{0.97}Ni_{5.06}$	0.14	0.22	5.0017	3.9915	86.48
0.4	$La_{0.95}Ni_{5.11}$	0.29	0.32	4.9940	3.9974	86.34

[a] Values are obtained from a linear interpolation from data reported in Ref. [9] for $x = 0$ and Ref. [21] for $x = 0.4$.

to that of a Ni dumbbell ($2 * 28 = 56$), it is difficult to accurately determine it from powder X-ray diffraction analysis. However this value can be obtained by EPMA. In addition, it can be estimated from the variations of the cell parameters that are very sensitive to x. Results using both methods are given in Table 2 for the three intermetallic compounds. A good agreement is observed between the nominal and the measured compositions for $x = 0$ and 0.2. As no extra phases could be observed in the diffraction patterns of these samples, it was concluded that the actual compositions correspond to the nominal ones. This is not the case for $x = 0.4$, for which a small amount of FCC Ni phase is observed in the diffraction patterns. Accordingly, the stoichiometry is expected to be lower than the nominal value. Indeed, refinement of the occupancy factors for nickel using the neutron data collected on the saturated deuteride leads to $x = 0.32$ in agreement with the value obtained from EPMA and cell variations. Therefore, the value of $x = 0.32$ was retained for this latter sample. As metal diffusion during hydriding is not expected to occur, the metal compositions for each other deuterated phases were kept fixed during the refinement of ND patterns to $x = 0$, 0.2 and 0.32 respectively. Details on the crystallographic structure of the intermetallic overstoichiometric phases can be found in Ref. [9].

Analysis of the diffraction pattern has been made first for the three saturated deuterides $LaNi_{5.0}D_{6.5}$, $La_{0.97}Ni_{5.06}D_{5.9}$ and $La_{0.95}Ni_{5.11}D_{5.45}$. The structure of the stoichiometric deuteride compound $LaNi_{5.0}D_{6.5}$ was correctly described using the seven-site model proposed by Lartigue et al. [15] in space group $P6_3mc$. Superstructure lines are clearly observed involving the doubling of the c-axis and a partial ordering of the deuterium atoms. Positions and occupancies of the different deuterium sites are given in Table 3. A good agreement is obtained between the refined deuterium amount (6.5 ± 0.5D/f.u.) and the value determined from the Sievert's method (6.5).

The superstructure lines were evidenced in the pattern of $La_{0.97}Ni_{5.06}D_{5.9}$ ($x = 0.2$) as shown in the inset of Fig. 2. Therefore, the same structural hypothesis as for $LaNi_{5.0}D_{6.5}$ was evaluated. Indeed, a good agreement was obtained between the observed and calculated patterns. Structural data for this compound are given in Table 3.

For $La_{0.95}Ni_{5.11}D_{5.45}$ ($x = 0.4$), none of the extra lines present in the two other deuterides were observed (Fig. 3). Therefore, simpler structural models were tested and the best agreement was obtained with the seven-site model in space group $P6mm$.

Following the determination of the structural properties of the saturated deuterides, analysis of the mid-plateau deuterides was performed. In agreement with the PCI curves, both α and β phases were found to coexist in the samples and refinement was made taking into account both compounds. Typical refined diffraction pattern is shown in Fig. 4. Careful examination of the data does not allow finding any superstructure lines as observed for $LaNi_{5.0}D_{6.5}$ and $La_{0.97}Ni_{5.06}D_{5.9}$. Therefore, a two-site ($6m$ and $12n$) model in space group $P6/mmm$ was assumed for the α phase and the seven-site model in space group $P6mm$, that is better adapted for the under-saturated deuterides, was used for the β phase. Detailed crystallographic data and applied constraints are given in Table 4.

As already mentioned, a peculiar attention was paid to the diffraction lines widths for all patterns. Indeed, severe anisotropic line broadening is observed for all compounds. Such feature is shown for example for $La_{0.97}Ni_{5.06}D_{5.9}$ in Fig. 5. In order to compare the broadening in the α phase and in the two deuterides β (in equilibrium with α) and β^+ (saturated), the parameters S_{AA} and S_{CC} are given in Table 5 and shown in Fig. 7.

4. Discussion

4.1. Metallic sub-lattices

Over-stoichiometry in the intermetallic compounds $LaNi_{5+x}$ involves a decrease of the cell volume as x increases. Correlatively, an increase of the plateau pressure and a reduced capacity are observed in the solid gas measurements (Fig. 6). These results are in good agreement with the data reported by Joubert et al. [9]. The structure of $LaNi_{5+x}$ can be correctly described by dumbbells of Ni atoms lying along the c-axis.

Table 3
Structural data for the saturated deuterides

	$P6_3mc$ model (2c)	$LaNi_5D_{6.5}$	$La_{0.97}Ni_{5.06}D_{5.9}$	$P6mm$ model (c)	$La_{0.95}Ni_{5.11}D_{5.45}$ (+1.8 wt% of FCC Ni phase)
$P6/mmm$ model (c)	Refined capacity (D/f.u.)	6.5(5)	6.2(3)	Refined capacity (D/f.u.)	5.6 (2)
	$a, 2.c$ (Å)	$a = 5.3954(3)$, $2.c = 8.5858(7)$	$a = 5.3610(3)$, $2.c = 8.5732(6)$	a, c(Å)	$a = 5.3281(3), c = 4.2752(2)$
	V/f.u. (Å^3)	108.22(1)	106.69(1)	V/f.u. (Å^3)	105.11(1)
	$\Delta V/V$	24.7%	23.4%	$\Delta V/V$	21.7%
La $1a$ $(0,0,0)$	La $2a(0,0,z)$	$z = 0.0156(8); n = 2(f)$	$z = 0.0158(9), n = 1.944(f)$	La $1a(0,0,z)$	$z = 0.042(2), n = 0.956(1)$
Ni $2c$ $(1/3,2/3,0)$	Ni $2b_1(1/3,2/3,0)$	$n = 2(f)$	$n = 1.833(f)$	Ni $2b(1/3,2/3,z)$	$z = 0(f), n = 1.738(1)$
	Ni $2b_2(1/3,2/3,1/2)$	$n = 2(f)$	$n = 1.833(f)$		
Ni $3g$ $(1/2,0,1/2)$	Ni $6c(1/2,0,1/4)$	$n = 6(f)$	$n = 6(f)$	Ni $3c(1/2,0,z)$	$z = \frac{1}{2}(f),\ n = 3(f)$
Ni 6ℓ $(x,2x,0)$	Ni $6c_1$ $(x,2x,0)$		$x = 0.267(f), n = 0.166(f)$	Ni $6e$ $(x,2x,z)$	$x = 0.267(6), z = 0(f), n = 0.262(1)$
	Ni $6c_2(x,2x,1/2)$		$x = 0.267(f), n = 0.166(f)$		
Ni $2e(0,0,z)$	Ni $2a_1(0,0,z/2)$		$z/2 = 0.13(f), n = 0.055(f)$	Ni $1a_1(0,0,z)$	$z = 0.26(11), n = 0.044(1)$
	Ni $2a_2(0,0,-z/2)$		$-z/2 = -0.13(f)$, $n = 0.055(f)$	Ni $1a_2(0,0,-z)$	$z = 0.26(11), n = 0.044(1)$
D $4h(1/3,2/3,z\approx0.36)$	$2b_1(1/3,2/3,z/2)$	Empty	Empty	$2b_1(1/3,2/3,z)$	Empty
	$2b_2$ $(1/3,2/3,z/2\ \frac{1}{2})$	Empty	Empty		
	$2b_3(1/3,2/3,-z/2)$	$-z/2 = -0.181(1)$, $n = 1.28(6)$	$-z/2 = -0.183(1)$, $n = 0.88(7)$	$2b_2(1/3,2/3,-z)$	$-z = -0.365(4), n = 0.56(2)$
	$2b_4$ $(1/3,2/3,\ -z/2-\frac{1}{2})$	$-z/2-\frac{1}{2} = -0.681(1)$, $n = 0.29(6)$	$-z/2-\frac{1}{2} = -0.683(1)$, $n = 0.42(7)$		
D $6m(x\approx0.15,2x,z=1/2)$	$6c_1(x,2x,z/2)$	$x = 0.139(1)$, $z/2 = 0.276(1), n = 3.2(2)$	$x = 0.143(1), z/2 = 0.288(1), n = 3.6(1)$	$6e(x,2x,z)$	$x = 0.142(1), z = 0.5(f)$, $n = 1.96(5)$
	$6c_2$ $(x,2x,\ z/2+\frac{1}{2})$	$x = 0.139(1)$, $z/2+\frac{1}{2} = 0.776(1)$, $n = 0.7(2)$	$x = 0.143(1)$, $z/2+\frac{1}{2} = 0.788(1)$, $n = 1.04(12)$		
D $12n(x\approx0.46,0,z\approx0.12)$	$12d_1(x,0,z/2)$	$x = 0.488(3), z/2 = 0.0528(3), n = 5.36(8)$	$x = 0.481(3), z/2 = 0.0539(3), n = 5.26(9)$	$6d_1(x,0,z)$	$x = 0.508(8)$, $z = 0.1095(9), n = 2.48(5)$
	$12d_2(x,0,-z/2)$	Empty	Empty	$6d_2(x,0,-z)$	Empty
D $12o(x\approx0.2,2x,z\approx0.35)$	$6c'_1(x,2x,z/2)$	Empty	Empty	$6e'_1(x,2x,z)$	Empty
	$6c'_2$ $(x,2x,\ z/2+\frac{1}{2})$	Empty	Empty		
	$6c'_3(x,2x,-z/2)$	$x = 0.200(8), -z/2 = -0.171(1), n = 0$	$x = 0.216(5), -z/2 = -0.147(3), n = 0.38(15)$	$6e'_2(x,2x,-z)$	$x = 0.24(f)$, $z = -0.342(6), n = 0.59(5)$
	$6c'_4$ $(x,2x,\ -z/2-\frac{1}{2})$	$x = 0.200(8)$, $-z/2-\frac{1}{2} = -0.671(1)$, $n = 2.3(2)$	$x = 0.216(5)$, $-z/2-\frac{1}{2} = -0.647(3)$, $n = 0.79(15)$		
	R factors (%)	$R_p = 1.9, R_{\omega p} = 2.3$, $\chi^2 = 2.9, R_{Bragg} = 2.9$	$R_p = 2.2, R_{\omega p} = 2.7$, $\chi^2 = 3.9, R_{Bragg} = 4.6$		$R_p = 2.4, R_{\omega p} = 3.2\chi^2 = 5.0, R_{Bragg} = 5.4$
	No of reflections	164	163		96

The three structural models are compared. The four-site model in space group $P6/mmm$ with a single c-axis, the 12-site model in space group $P6_3mc$ with a doubled c-axis and the seven-site model in space group $P6mm$ with a single c-axis are described. Estimated standard deviations are given between brackets; occupancy parameters (n) are given in atom per cell; (f) stands for fixed parameters. $\Delta V/V$ corresponds to the volume expansion between the intermetallic compound and the deuteride. For the compound $La_{0.95}Ni_{5.11}D_{5.45}$ the over-stoichiometry of the metallic sub-lattice was refined using the following constraints: La $1a(1-y)$, Ni $2b(2-6y)$, Ni $6e(6y)$, Ni $1a_1$ and $1a_2(y)$.

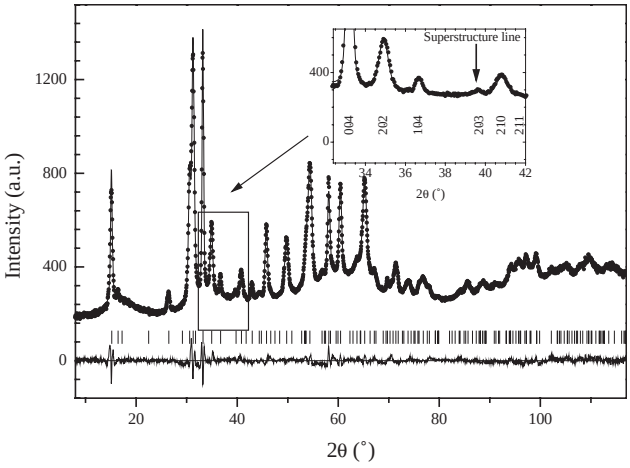

Fig. 2. Refined neutron diffraction pattern for $La_{0.97}Ni_{5.06}D_{5.9}$ (observed (•), calculated (—) and difference (below) patterns). The inset shows one of the superstructure lines (203) involving the doubling of the *c*-axis.

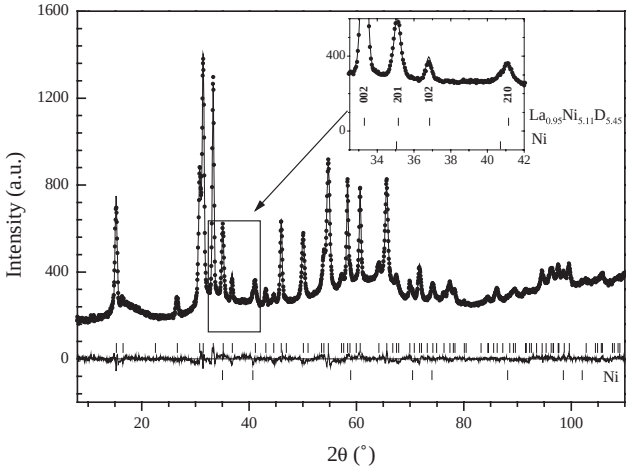

Fig. 3. Refined neutron diffraction pattern for $La_{0.95}Ni_{5.11}D_{5.45}$ (observed (•), calculated (—) and difference (below) patterns). The inset shows the absence of any visible superstructure line by comparison to $La_{0.97}Ni_{5.06}D_{5.9}$.

Accordingly, this model was retained for the metallic substructure of the deuterides and it was assumed that no significant changes occur for the metallic lattice by hydrogen loading. However, descriptions in *P6mm* or $P6_3mc$ space group allow both refining the *z* position of the La atoms (1*a* in *P6mm* and 2*a* in $P6_3mc$). Such refinement leads to a small positive shift of the La atoms along the *c*-axis (Table 3). Nickel atoms occupy the same positions as in the parent $CaCu_5$ structure type.

4.2. α Phases

For all values of *x*, the α phases are correctly described in the *P6/mmm* space group. As reported in

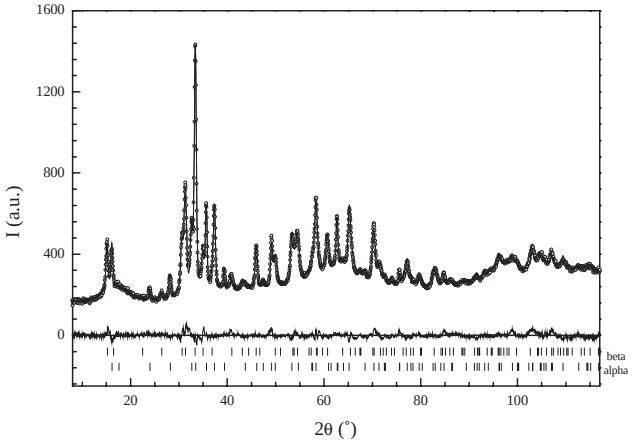

Fig. 4. Refined neutron diffraction pattern for the mid plateau deuteride $La_{0.97}Ni_{5.06}D_3$ (observed (•), calculated (—) and difference (below) patterns). Both α (bottom) and β (top) phases are shown by vertical ticks.

previous works on related AB_5 compounds [11,22], deuterium is found to lie in sites 6*m* and 12*n*. Despite the difficulties in refining coexisting α and β phases, a good agreement is obtained with this structural model, whatever the stoichiometry *x*. Our results are also in agreement with the data published by Soubeyroux et al. [23] that report on hydrogen in site 12*n* and possible occupation of site 6*m* for the compounds $LaNi_5D_{0.3}$.

If the structural model remains the same whatever the values of *x*, occupancy factors are significantly different. The D concentration increases from 0.42(4) D/f.u. for $x = 0-0.72(6)$ D/f.u. for $x = 0.4$ and this capacity increase is observed at both sites. Accordingly, the cell volume variation increases from 0.74% to 1.14%.

4.3. β Phases in equilibrium with α ones

All β phases in equilibrium with α can be described with the same hexagonal symmetry in the *P6mm* space group. Compared to the *P6/mmm* model, this structural description corresponds to a redistribution of the deuterium atoms along the *c*-axis, a loss of the mirror and a splitting of the deuterium sites (4*h*, 6*m*, 12*n*, 12*o*) into seven (Table 3 and Fig. 1). According to the literature, the *P6mm* space group has already been reported by Lartigue et al. [15] for $LaNi_5D_5$ at 90°C and by Joubert et al. for $LaNi_{4.8}Sn_{0.2}D_{6.1}$ [24] and $LaNi_{4.75}Pt_{0.25}D_{5.23}$ [25] at room temperature whereas other substituted deuteride compounds $LaNi_{5-z}M_zD_w$ (M = Mn, Fe, Al, Si, Ge) adopt the *P6/mmm* symmetry [26,27]. According to these results, the conclusion can be drawn that for binary $LaNi_5$ or for a very low substitution rate, the D ordering along the *c*-axis occurs for larger substitution rate, the *P6/mmm* symmetry is retained. This is in agreement with the present work as the over-stoichiometric compounds $La_{1-y}Ni_{5+2y}$ are

Table 4
Structural data for the mid-plateau deuterides

Nominal composition	$LaNi_5D_{2.95}$	$La_{0.97}Ni_{5.06}D_{3.0}$	$La_{0.95}Ni_{5.11}D_{2.98}$
α Phase ($P6/mmm$)	wt% = 63%	wt% = 54%	wt% = 59%
Refined capacity	0.42(4) D/f.u.	0.57(6) D/f.u.	0.72(6) D/f.u.
a, c (Å), V (Å^3)	$a = 5.0277(3), c = 3.9946(6), V = 87.44(1)$	$a = 5.0252(5), c = 3.9966(3), V = 87.40(1)$	$a = 5.0230(3), c = 3.9967(2), V = 87.33(1)$
$\Delta V/V$	0.74%	1.06%	1.14%
La $1a(0,0,0)$		$n = 0.972(f)$	$n = 0.956(f)$
Ni $2c(1/3,2/3,0)$		$n = 1.833(f)$	$n = 1.738(f)$
Ni $3g(1/2,0,1/2)$		$n = 3(f)$	$n = 3(f)$
Ni $6\ell(x,2x,0)$		$x = 0.267(f), n = 0.167(f)$	$x = 0.267(f), n = 0.262(f)$
Ni $2e(0,0,z)$		$z = 0.26(f), n = 0.056(f)$	$z = 0.26(f), n = 0.088(f)$
D $6m(x,2x,1/2)$	$z = 0.146(f), n = 0.10(2)$	$z = 0.143(f), n = 0.15(3)$	$z = 0.142(f), n = 0.18(3)$
D $12n(x,0,z)$	$x = 0.480(f), z = 0.111(1), n = 0.32(2)$	$x = 0.48(f), z = 0.108(f), n = 0.42(3)$	$x = 0.48(f), z = 0.11(4), n = 0.54(3)$
	$R_{\mathrm{Bragg}} = 5.6$	$R_{\mathrm{Bragg}} = 7.2$	$R_{\mathrm{Bragg}} = 6.1$
β phase ($P6mm$)	wt% = 37%	wt% = 46%	wt% = 41%
Refined capacity	6.2(4) D/f.u.	5.9(3) D/f.u.	5.2(3) D/f.u.
a, c (Å), V (Å^3)	$a = 5.3828(5), c = 4.2744(4), V = 107.36(1)$ Å^3	$a = 5.3483(5), c = 4.2665(5), V = 105.69(2)$ Å^3	$a = 5.3144(4), c = 4.2541(4), V = 104.05(1)$ Å^3
$\Delta V/V$	23.7%	22.2%	20.5%
La $1a$ $(0,0,0)$	$z = 0(f), n = 1(f)$	$z = 0.052(2), n = 0.972(f)$	$z = 0.036(2), n = 0.956(f)$
Ni $2b(1/3,2/3,z)$	$z = 0(f), n = 2(f)$	$z = 0(f), n = 1.833(f)$	$z = 0(f), n = 1.738(f)$
Ni $3c(1/2,0,z)$	$z = \frac{1}{2}(f),\ n = 3(f)$	$z = \frac{1}{2}(f),\ n = 3(f)$	$z = \frac{1}{2}(f),\ n = 3(f)$
Ni $6e(x,2x,z)$		$x = 0.267(f), z = 0(f), n = 0.167(f)$	$x = 0.267(f), z = 0(f), n = 0.262(f)$
Ni $1a_1(0,0,z)$		$z = 0.26(f), n = 0.028(f)$	$z = 0.26(f), n = 0.044(f)$
Ni $1a_2(0,0,-z)$		$z = 0.26(f), n = 0.028(f)$	$z = 0.26(f), n = 0.044(f)$
D $2b_2(1/3,2/3,-z)$	$z = -0.346(8), n = 0.49(3)$	$z = -0.366(f), n = 0.59(4)$	$z = -0.365(f), n = 0.45(5)$
D $6e(x,2x,z)$	$x = 0.146(f), z = 0.50(f), n = 1.62(8)$	$x = 0.143(f), z = 0.50(f), n = 1.94(9)$	$x = 0.142(f), z = 0.50(f), n = 1.77(9)$
D $6d_1(x,0,z)$	$x = 0.48(f), z = 0.111(1), n = 2.78(10)$	$x = 0.485(f), z = 0.108(f), n = 2.57(9)$	$x = 0.512(f), z = 0.109(f), n = 2.69(9)$
D $6e'_1(x,2x,z)$	$x = 0.21(f), z = 0.364(6), n = 0.16(9)$	$n = 0$	$n = 0$
D $6e'_2(x,2x,-z)$	$x = 0.21(f), z = -0.364(6), n = 1.16(11)$	$x = 0.21(f), z = -0.298(f), n = 0.79(9)$	$x = 0.24(f), z = -0.341(f), n = 0.31(9)$
	$R_{\mathrm{Bragg}} = 5.8$	$R_{Bragg} = 8.1$	$R_{\mathrm{Bragg}} = 9.2$
Total refined in D/f.u.	2.6 D/f.u.	3.0 D/f.u.	D: 2.6 D/f.u.
Discrete vol. expansion	22.8%	20.9%	19.1%
R factors (%)	$R_{\mathrm{p}} = 2.3, R_{\omega\mathrm{p}} = 2.7, \chi^2 = 3.5$	$R_{\mathrm{p}} = 2.4, R_{\omega\mathrm{p}} = 3.0, \chi^2 = 4.2$	$R_{\mathrm{p}} = 2.7, R_{\omega\mathrm{p}} = 3.2, \chi^2 = 4.9$
No of reflections	82(α)/97(β)	82(α)/98(β)	82(α)/94(β)

Space group $P6/mmm$ with two site model was retained for the alpha phase whereas the seven-site model in space group $P6mm$ with a single c-axis was used for the beta phase in equilibrium on the plateau. Estimated standard deviations are given between brackets; (f) stands for fixed parameters. Position and occupancy factors for metallic atoms were fixed to the value used for the saturated deuterides.

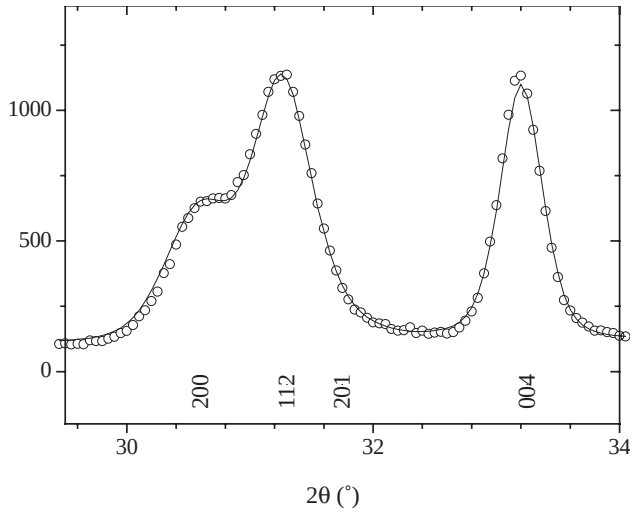

Fig. 5. Selected region of the diffraction pattern (observed (dots) and refined (full line)) showing anisotropic line broadening in the deuteride $La_{0.97}Ni_{5.06}D_{5.9}$ for several $h\,k\,l$ lines. The anisotropic broadening is particularly visible from the comparison of 2 0 0 and 0 0 4 lines.

Table 5
Strain parameters S_{AA} and S_{CC} (10^{-3} Å^{-2}) in the basal plane and along the c-axis of the hexagonal cell allowing the description of the anisotropic line broadening for the α phase and for the two deuterides (β in equilibrium with α and β^+ (saturated))

Phase	Strain parameter	$LaNi_5$	$La_{0.97}Ni_{5.06}$	$La_{0.95}Ni_{5.11}$
α	S_{AA}	0.613(5)	0.558(6)	0.453(5)
	S_{CC}	0.253(6)	0.262(7)	0.160(6)
β	S_{AA}	0.762(9)	0.603(7)	0.439(6)
	S_{CC}	0.302(9)	0.343(11)	0.251(9)
β^+	S_{AA}	0.794(4)	0.629(4)	0.424(4)
	S_{CC}	0.078(5)	0.070(1)	0.146(5)

very close to the binary stoichiometric one. However, if the structural models are identical, D occupancies are significantly different between the compounds: the total D content decreases from 6.2(4) D/f.u. for $x = 0$ down to 5.2(3) D/f.u. for $x = 0.4$. Total volume expansion varies from 23.7% down to 20.5%, respectively. From the neutron diffraction data analysis, it appears that the capacity loss is almost exclusively related to the decrease of sites $6e'_1$ and $6e'_2$ (equivalent to 12o in $P6/mmm$) occupancies whereas other site occupancies are nearly constant.

4.4. β Phases in solid solution branch

For the deuterides studied in the solid solution domain, all compounds can be described in hexagonal symmetry. However, depending of x, two different cases are observed. For $LaNi_5$ and $La_{0.97}Ni_{5.06}$ ($x = 0.2$) superstructure lines are present, involving a doubling of the c-axis and a correct description is obtained in space group $P6_3mc$. Again this structural change can be explained by deuterium rearrangement along the c-axis as it was proposed by Lartigue et al. [18] for $LaNi_5D_{6.7}$, by Latroche et al. for $LaNi_4CoD_{6.11}$ [19] and by Thompson et al. [16] for $LaNi_5D_7$. The long-range order implies the doubling of the cell along the c-axis due to different D site occupancy factors. Appearance of ordering can be directly related to the increase of the deuterium content. In the present work, occupancy factors for stoichiometric $LaNi_5$ are in rather good agreement with those reported by Lartigue. However a higher filling of the sites 6c (equivalent to 6m in $P6/mmm$ s.g.) at the expense of the sites 6c' (equivalent to 12o) is observed in our work. Moreover, refinement of the z position for site 6c (which was not refined by Lartigue) leads to a small shift above the plane $z = 1/4$ and $z = 3/4$. This has to be related to the small shift also observed for the lanthanum atom above the origin position.

For $x = 0.4$, no superstructure lines can be detected and the pattern can be correctly refined in the $P6mm$ space group without doubling the c parameter. However, it cannot be excluded that a doubling of the cell related to deuterium ordering may appear at higher deuterium pressure (i.e., larger deuterium concentration) for this latter compound. As a matter of fact, the progressive transformation (corresponding to D atoms ordering) from $P6mm$ to $P6_3mc$ subgroup can be achieved either by increasing the hydrogen capacity or by decreasing the over-stoichiometry.

According to this work, the deuterium concentration in the β phase decreases from 6.5(5) D/f.u. ($x = 0$) to 6.2(3) D/f.u. ($x = 0.2$) and 5.6(2) D/f.u. ($x = 0.4$). As the samples were prepared in similar conditions (saturated at about 10 bar D pressure at 25°C), these capacities can be directly compared. Between the two samples with a double cell, the capacity reduction is mainly due to a reduced filling of sites $6e'_1$ and $6e'_2$ (equivalent to 12o in $P6/mmm$) but for the compound with $x = 0.4$ described in a single cell, the capacity decrease is mainly due to a poorer filling of site 6e (equivalent to 6m in $P6/mmm$).

4.5. Comparison with solid gas data

A rather good agreement is obtained between the data from volumetric measurements and the refined concentrations deduced from neutron data analysis as shown in Figs. 6a–c. The effects of x on the structural and thermodynamic properties are important. The plateau width is reduced from 5.8(8) D/f.u. for $x = 0$–4.5(9) D/f.u. for $x = 0.4$. This is due to both an increase of the maximum concentration of the α phase and a decrease of the minimum capacity of the β one. Correlatively, the so-called discrete volume expansion (i.e., the volume variation at the α–β transition) decreases linearly with x

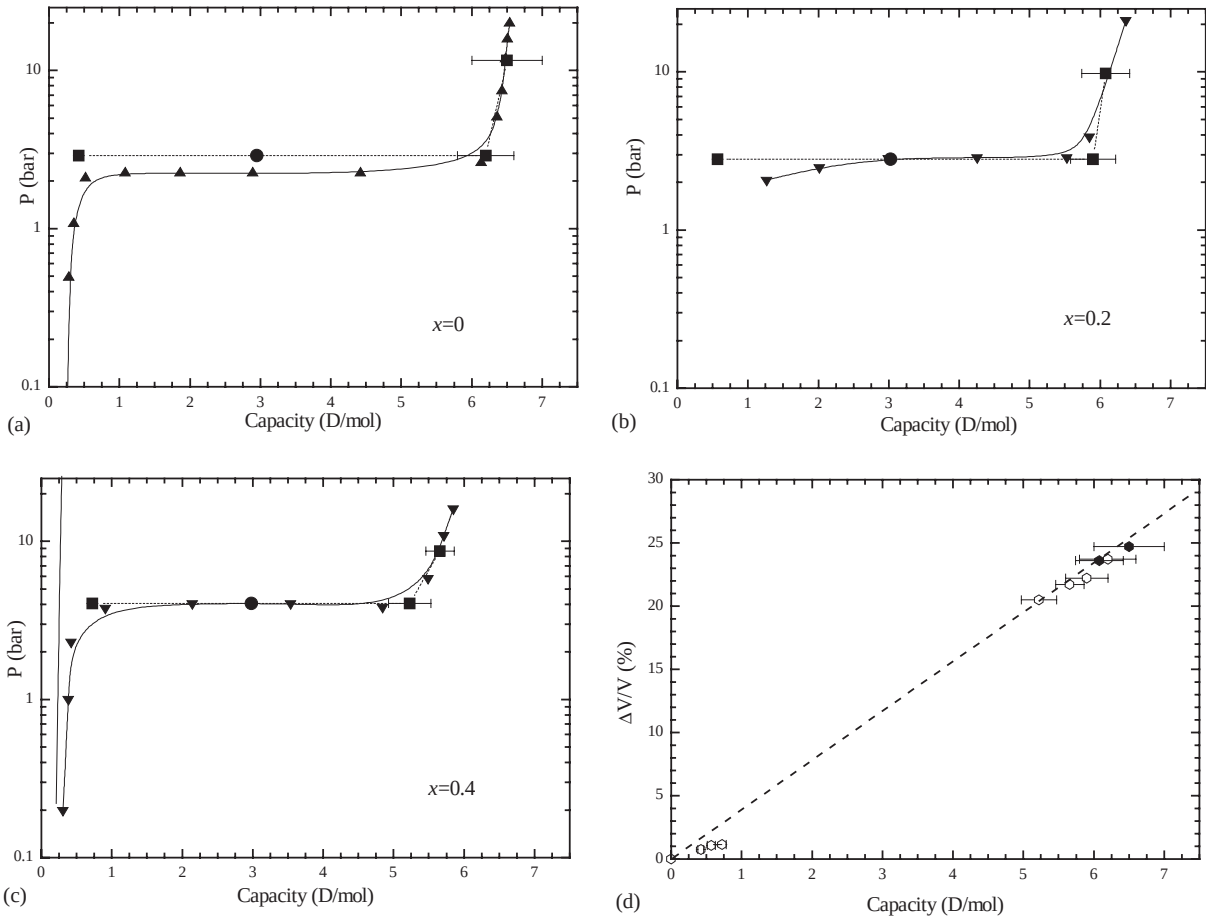

Fig. 6. Comparison between the data obtained by solid gas measurements (triangle + full line) and the capacity determined by neutron diffraction analysis (full squares): (a) for $x = 0$ (absorption); (b) for $x = 0.2$ (desorption); (c) for $x = 0.4$ (desorption), the samples prepared for the mid-plateau analysis are shown as a full circle on the plot; (d) evolution of the volume expansion as a function of the deuterium content (hexagonal symbols for $P6/mmm$, open circles for $P6mm$ and full circles for $P6_3mc$, dashed line is only a guide for eyes).

from 22.8% down to 19.1%. It is worth to note that the total volume expansion (i.e., volume change between intermetallic and deuterides) increases linearly with D content and is independent of the symmetry ($P6mm$ or $P6_3mc$) as shown in Fig. 6d. However, volume expansion in the α phase is lower than what can be expected assuming a linear increase of $\Delta V/V$. Such behavior has already been observed in other systems like $LaNi_{4.6}Ge_{0.4}$–D system [27]. It is possibly related to the fact that only two sites are occupied in the α phase ($6m$ and $12n$).

4.6. Anisotropic line broadening

Line profile analysis provides valuable informations on the strains induced by hydrogen absorption in the different samples. Anisotropic line broadening is correctly described using the two parameters S_{AA} and S_{CC}. In all cases, S_{AA} is significantly larger than S_{CC} (Fig. 7). The values obtained in this work are in good agreement with data reported by Cerný et al. [20] who found $S_{AA} = 0.76 \times 10^{-3}$ Å^{-2} and $S_{CC} = 0.22 \times 10^{-3}$ Å^{-2} for a stoichiometric compound $LaNi_5$ and $S_{AA} = 0.59 \times 10^{-3}$ Å^{-2} and $S_{CC} = 0.18 \times 10^{-3}$ Å^{-2} for a compound with $x = 0.2$. However, those data were obtained on desorbed samples (deuterium loaded in our case) after 15 cycles (versus 5 cycles for the present work) and it is expected that such strain parameters can evolve during cycling process. Nevertheless, our data confirms the observations made by Cerný et al. [20]: strain parameter S_{AA} decreases when the stoichiometry parameter x increases. The behavior of S_{CC} is less obvious as this parameter is almost constant or even increases for the saturated deuteride $La_{0.95}Ni_{5.11}D_{5.45}$ but it is very probable that additional hydrogen uptake would induce a transformation to space group $P6_3mc$ and a reduction of the strain parameter. Moreover, the difference between S_{AA} and S_{CC} is also reduced with x, leading to less anisotropic broadening. It is worth noting that the overall reduction of the strain parameters is well correlated with the diminution of the discrete lattice volume expansion $\Delta V/V$, this confirms

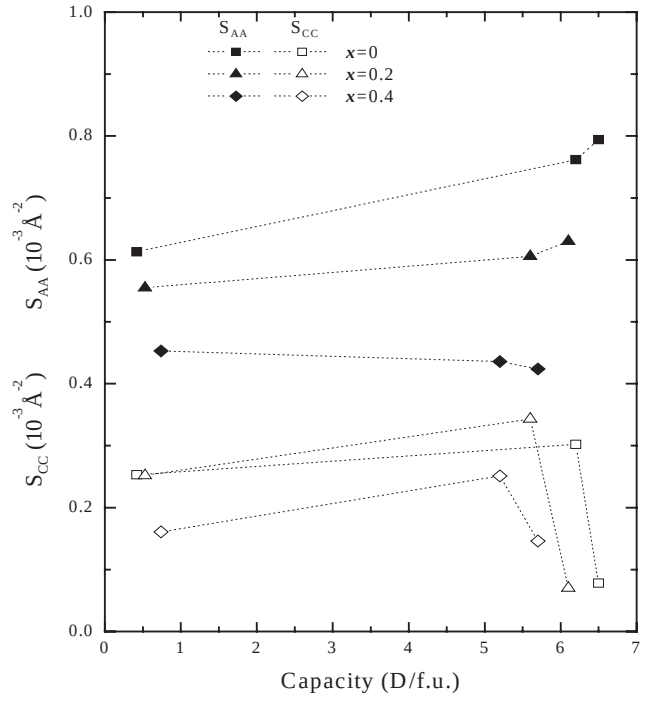

Fig. 7. Evolution of the strain parameters S_{AA} (full symbol) and S_{CC} (open symbol) as a function of the D capacity for the $LaNi_{5+x}$ compounds with $x = 0$ (square), 0.2 (triangle) and 0.4 (diamond).

that most of the defects are created when crossing the two-phase region.

On the contrary to Cerný et al. [20] that measured the strain parameters on desorbed samples, our data allows to follow the evolution of the strain parameters as a function of the hydrogen content. Relatively weak variations are observed on the plateau and even in the β branch for S_{AA}. This is no longer the case for S_{CC} that slightly increases on the plateau, before to be strongly reduced for all x values within the β branch. This unexpected behavior cannot be correlated to any anisotropic effect from the variation of the cell parameters since both of them vary almost linearly as a function of the deuterium content. However, in order to recover the values observed for S_{AA} and S_{CC} in the alpha phases or even in the desorbed samples, it can be concluded that defects are created and removed within the hydrogenation cycling process. These results must be compared to those of Wu et al. [28] that studied in situ the first hydrogenation of stoichiometric $LaNi_5$ by means of synchrotron radiation. According to these authors, the dislocation structure is inheritable during the α–β phase transition and dislocations are formed mainly from the nucleation and growth of the β phase, all being retained during subsequent phase transitions. From our work and according to the peculiar variation of S_{CC} in the β branch, a reversible defect loop cannot be excluded upon cycling.

It can be proposed that the better cycle life observed for over-stoichiometric samples is related to the overall reduction of the strains created during cycling process leading to less defects in the material and thus to a reduced decrepitation, a phenomenon responsible for high corrosion of those compounds when used as electrode materials. All together, these various parameters (discrete volume expansion, strain anisotropy and strain density) are lowered with x, leading to less brittle materials.

5. Conclusions

The crystal structures of the different phases (α and β at equilibrium with α and saturated β) have been determined as a function of the over-stoichiometry x for the deuterides $LaNi_{5+x}D_y$ ($x = 0$; 0.2 and 0.4). For the β phases in equilibrium with α, the capacity loss with x is attributed to a lower filling of sites $6e'_1$ and $6e'_2$. The behavior for $x = 0.2$ can be closely related to that of the binary stoichiometric compound $LaNi_5$ whereas for $x = 0.4$ the D atom ordering involving a doubling of the cell parameter along the c-axis is not observed. The progressive transformation from $P6mm$ to $P6_3mc$ subgroup corresponding to D atoms ordering can be achieved either by increasing the hydrogen capacity or by decreasing the over-stoichiometry (x).

Anisotropic line broadening analysis shows that strains are reduced with over-stoichiometry x. This effect can be related to the reduction of the plateau width attributed to a D richer α phase and a poorer β one. The compound with $x = 0.4$ shows much isotropic behavior that the two other ones that may explain the better cycle life observed for over-stoichiometric compounds when submitted to long-term absorption–desorption processes.

Acknowledgments

The authors wish to thank Mrs. F. Briaucourt and Mr. E. Leroy for technical assistance.

References

[1] R.C. Bowman Jr., C.H. Luo, C.C. Ahn, C.K. Witham, B. Fultz, J. Alloys Compd. 217 (1995) 185.
[2] P.H.L. Notten, J.L.C. Daams, R.E.F. Einerhand, Ber. Bunsenges. Phys. Chem. 96 (5) (1992) 656.
[3] P.H.L. Notten, J.L.C. Daams, R.E.F. Einerhand, J. Alloys Compd. 210 (1994) 233.
[4] P.H.L. Notten, R.E.F. Einerhand, J.L.C. Daams, J. Alloys Compd. 210 (1994) 221.
[5] P.H.L. Notten, R.E.F. Einerhand, J.L.C. Daams, Z. Phys. Chem. 183 (1994) 267.

[6] P.H.L. Notten, M. Latroche, A. Percheron-Guégan, J. Electrochem. Soc. 146 (1999) 3181.
[7] K.H.J. Buschow, H.H. Van Mal, J. Less-Common Met. 29 (1972) 203.
[8] D. Zhang, J. Tang, K.A. Gschneidner Jr., J. Less-Common Met. 169 (1) (1991) 45.
[9] J.-M. Joubert, R. Cerný, M. Latroche, E. Leroy, L. Guénée, A. Percheron-Guégan, K. Yvon, J. Solid State Chem. 166 (1) (2002) 1.
[10] J.-C. Achard, F. Givord, A. Percheron-Guégan, J.-L. Soubeyroux, F. Tasset, J. Phys. C5 40 (1979) 218.
[11] M. Latroche, A. Percheron-Guégan, F. Bourée-Vigneron, J. Alloys Compd. 265 (1–2) (1998) 209.
[12] F. Cuevas, M. Hirscher, B. Ludescher, H. Kronmuller, J. Appl. Phys. 86 (12) (1999) 6690.
[13] F. Cuevas, M. Latroche, M. Hirscher, A. Percheron-Guégan, J. Alloys Compd. 323–324 (2001) 4.
[14] F. Cuevas, J.-M. Joubert, M. Latroche, O. Isnard, A. Percheron-Guégan, Appl. Phys. A 74 (2002) S1175.
[15] C. Lartigue, A. Percheron-Guégan, J.-C. Achard, J.-L. Soubeyroux, J. Less-Common Met. 113 (1985) 127.
[16] P. Thompson, J.J. Reilly, L.M. Corliss, J.M. Hastings, R. Hempelmann, J. Phys. F. Met. Phys. 16 (1986) 675.
[17] J. Rodríguez-Carvajal, XV Congress of International Union of Crystallography, Satellite Meeting on Powder Diffraction Toulouse, France, 1990, p. 127.
[18] C. Lartigue, A. Lebail, A. Percheron-Guégan, J. Less-Common Met. 129 (1987) 65.
[19] M. Latroche, J. Rodríguez-Carvajal, A. Percheron-Guégan, F. Bourée-Vigneron, J. Alloys Compd. 218 (1) (1995) 64.
[20] R. Cerný, J.-M. Joubert, M. Latroche, A. Percheron-Guégan, K. Yvon, J. Appl. Crystallogr. 33 (2000) 997.
[21] M. Latroche, J.-M. Joubert, A. Percheron-Guégan, P.H.L. Notten, J. Solid State Chem. 146 (1999) 313.
[22] J.-M. Joubert, M. Latroche, A. Percheron-Guégan, F. Bourée-Vigneron, J. Alloys Compd. 275–277 (1998) 118.
[23] J.L. Soubeyroux, A. Percheron-Guégan, J.-C. Achard, J. Less-Common Met. 129 (1987) 181.
[24] J.-M. Joubert, M. Latroche, R. Cerný, R.C. Bowman Jr., A. Percheron-Guégan, K. Yvon, J. Alloys Compd. 293–295 (1999) 124.
[25] J.-M. Joubert, J. Charton, A. Percheron-Guégan, J. Solid State Chem. 173 (2003) 379–386.
[26] A. Percheron-Guégan, C. Lartigue, Mater. Sci. Forum 31 (1988) 125.
[27] J.-M. Joubert, M. Latroche, R.C. Bowman, A. Percheron-Guégan, F. Bourée-Vigneron, Appl. Phys. A 74 (Sup. Part II) (2002) S1037.
[28] E. Wu, E.M.A. Gray, D.J. Cookson, J. Alloys Compd. 330–332 (2002) 229.